I R A M P
4(1), June 2013, pp. 29-47

ISSN: 2229-3159

Doubly Excited States under Spherical Confinement: A Case Study

SUBHRANGSU SEN[1,4], PUSPAJIT MANDAL[1], PRASANTA KUMAR MUKHERJEE[1,2] AND BURKHARD FRICKE[3]

[1]Department of Mathematics, Visva-Bharati, Santiniketan 731 235, West Bengal, INDIA
[2]Department of Physics, Ramakrishna Mission Vivekananda University, Belur Math, Howrah 711 202 West Bengal, INDIA
[3]Institute of Physics, University of Kassel D 34109 Kassel, GERMANY
[4]Patha-Bhavana, Visva-Bharati, Santiniketan 731 235, West Bengal, INDIA

ABSTRACT: The effect of spherical confinement on the doubly excited states of *He* atom bounded below the ionization threshold of He^+ corresponding to n = 2, 3 and 4 have been analyzed using radially correlated product basis sets The motivation is to understand the structural behavior of such states under the thermodynamic pressure generated due to such confinements. Helium is chosen as a prototype system as it is the simplest two electron system for which spectroscopic observations are abundant. The general observation is that the number of doubly excited states diminish as radius of confinement decreases with consequent increase of the double excitation energy of various configurations from the ground state. A general enhancement of the average value of Coulomb repulsion term is observed with increase of confinement. The three dimensional plots of the density of doubly excited states of different symmetries with respect to radial distance show consistent behavior of the nodes, the peak positions of the density profiles and their heights with respect to the radius of spherical confinement

1. INTRODUCTION

The concept of spherical confinement was first introduced by Michels *et al* [1] and later on by Sommerfeld and Welker [2] where they studied in detail the binding energy and polarizability of hydrogen atom inside a spherical box with varying radius. Nature provides example of such spatially confined systems with atoms and molecules in Zeolite sieves [3, 4], fullerenes [5-9], solutes under solvent environments [10-12] and storage of ions in specific solids [13]. A review on different forms of confined systems, interpretation of their energy levels and other properties have been discussed by Jaskolski [14] and by Sil *et al* [15]. The obvious effect of spherical confinement is to produce an altered boundary condition on the wave function which must be taken care of while solving the Schrödinger equation of the system. Detailed non-relativistic studies of the stability of the ground and single excited states and other structural properties like the ionization radii, electric dipole polarizabilities, hyperfine effect etc. for H atom under spatial confinement have been performed by different workers using various methods [16-32]. A relativistic approach towards the stability of confined H atom was due to Huang *et al* [33]. Attempts for such studies on two and many electron systems are however limited [34-38]. The overall inferences drawn from such calculations so far are the gradual instability of the ground and excited state energy levels, reduction of ionization potential and polarizabilities, formation of quantum chaos under confinement, orbital collapses and intercrossing of orbitals of different symmetries modifying thereby the atomic shell structure [34-38]. Under very strong confinement the behavior of the system is expected to be completely controlled by the cavity only. The only calculation available for the lowest doubly excited *S* state of helium under spherical confinement was due to Chakraborty and Ho [39] who established their autoionizing character by calculating their widths. They used a suitable potential to simulate such a confinement and estimated the energy level and width of the lowest lying autoionizing *S* state of helium under different confining potential which vanishes asymptotically.

Presently our aim is to study the energy levels and electron density profiles of doubly excited states of He under external spherical confinement. We have investigated the behavior of the doubly excited energy levels, the Coulomb repulsion in these states and in particular the structural profiles of the two particle density function against the radii of confinement. Specifically we have chosen the doubly excited *nsn's* : $^1S^e$, *npn'p* :$^1D^e$, *ndn'd* :$^1G^e$ (n = 2, 3, 4; n' = n, n+1, …, 4) for our study and used only radially correlated basis sets for the description of such states. Essentially these doubly excited states are bounded below n = 2, 3, 4 respectively of the corresponding He^+ ion under identical confinement. Under spherical confinement the degeneracy of the hydrogenic levels with respect to orbital angular momentum for a given principal quantum number is lifted. In calculating the bounds the lifting of the degeneracy has been taken care of. A brief outline of the theory is given in section 2 followed by a discussion of the results in section 3.

2. THEORY

We consider a two electron system initially in its ground state described by the usual non relativistic Hamiltonian H_0. The system is confined in a spherical cavity of radius R. The ground state energy E_0 is determined from the solution of the Schrödinger equation

$$H_0\Psi = E_0\Psi \tag{1}$$

subject to

$$\langle\Psi \mid \Psi\rangle = 1 \tag{2}$$

We use a.u. throughout and obtain E_0 for a given value of R by imposing the finite boundary condition on the radial part of the ground orbitals so that no electron current takes place through the bounding surface [40] *i.e.*

$$\psi(r) = 0 \text{ at } r \geq R \tag{3}$$

and

$$\int_0^R \left|\psi(r)\right|^2 r^2 dr = 1 \tag{4}$$

here $\psi(r)$ is radial part of the one particle function constituting Ψ.

The boundary condition can be satisfied by expanding the radial part $\psi(r)$ in terms of a Slater basis set $\chi(r)$ given by

$$\psi(r) = (R - r)\,\chi(r) \tag{5}$$

with

$$\chi(r) = \sum_i C_i r^{n_i} e^{-\rho_i r} \tag{6}$$

here C's are linear variation parameters and n_i, ρ_i are pre assigned exponents. The ground state energy for a given value of R is obtained by solving the generalized eigen value equation

$$\underline{\underline{H_0}}\,\underline{C} = E_0\,\underline{\underline{S}}\,\underline{C} \tag{7}$$

where $\underline{\underline{H_0}}$ is the Hamiltonian matrix over the basis set and $\underline{\underline{S}}$ is the overlap matrix. To study the doubly excited states of the system under such a spherical confinement, time evolution of the ground state Ψ under a harmonic perturbation

$$H'(\underline{r},t) = G(\underline{r})e^{-i\omega t} + G^+(\underline{r})e^{i\omega t} \tag{8}$$

is analyzed. Here $G(\underline{r})$ is a two particle operator having permutation symmetry in radial as well as angular co-ordinates of the two electrons and may be expressed as

$$G(\underline{r}) = \lambda\left[f\left(\underline{r}_1, \underline{r}_2\right) + f\left(\underline{r}_2, \underline{r}_1\right)\right] \tag{9}$$

where λ is the perturbation strength parameter and $f\left(\underline{r}_1, \underline{r}_2\right)$ is conveniently expressed as a product of one particle operators

$$f\left(\underline{r}_1, \underline{r}_2\right) = h\left(\underline{r}_1\right)h'\left(\underline{r}_2\right) \tag{10}$$

where we have chosen

$$h(\underline{r}) = r^l Y_{lm}(\theta, \varphi) \tag{11}$$

in which the magnetic quantum number m is restricted to $|l|$.

This particular choice for both the one particle operators ensures simultaneous excitations of both the electrons with multipolarity l such that the total angular momentum of the doubly excited states $L = l+l$. The choice of $m = |l|$ excludes the possibility of generation of angular momentum $L < l + l$. Hence configuration mixing from the angular momentum states due to Russell Saunders coupling does not arise. In case of our specific study of excitations of identical symmetry from both the orbitals of the ground state, $l = 0$, 1 or 2 is chosen for both the operators ensuring $1s^2$:$^1S^e$: *nsn's* :$^1S^e$, *npn'p* :$^1D^e$ and *ndn'd* :$^1G^e$ states The total wavefunction in presence of the periodic perturbation may be expressed as [up to first order]

$$\Phi(\underline{r}, t) = N\left[\Psi(\underline{r}) + \delta\Psi^{-}(\underline{r})e^{-i\omega t} + \delta\Psi^{+}(\underline{r})e^{i\omega t}\right]e^{-iE_0 t} \tag{12}$$

where the normalization constant N is determined up to second order from the time averaged ansatz

$$\frac{1}{T}\int_0^T \left\langle \Phi(\underline{r}, t) \middle| \Phi(\underline{r}, t) \right\rangle dt = 1 \tag{13}$$

Here the time averaging is performed over the period of the oscillatory perturbation. The quantity $e^{-iE_0 t}$ describes the time evolution of the ground state in absence of external perturbation and $\delta\Psi^{\pm}e^{\pm i\omega t}$ furnish the first order corrections to the ground state wavefunction due to the two components of the perturbation given by eqn. (8). The nature of $\delta\Psi^{\pm}$ is obtained from

$$\delta\Psi^{\pm}(\underline{r}) \sim G(\underline{r})\Psi(\underline{r}) \tag{14}$$

The angular character of $\delta\Psi^{\pm}$ is given by eqn. (14), while the radial part is expanded in terms of product basis sets

$$\delta\Psi^{\pm}(\underline{r}) = \sum_j D_j^{\pm}\eta_j(1,2) \tag{15}$$

in which $D_j^{\pm}$ are the expansion coefficients and the two particle basis $\eta_j(1,2)$ is obtained from products of appropriate one particle Slater type basis

$$\eta_j(1,2) \sim \xi_k(1)\xi_l'(2) + \xi_l'(1)\xi_k(2) \tag{16}$$

The angular part of the STO's is so chosen as to obtain the angular character of the two particle wave function. In case of excitations having identical symmetry of both the excited orbital's the sets comprising ξ and ξ' are

identical and the number of independent coefficients $D^{\pm}$ will be $N(N + 1)/2$ where N is the number of STO's representing the one particle orbital. Further to ensure finite boundary condition on the excited orbitals the radial part of the orbitals $\xi(r)$ is represented as

$$\xi(\underline{r}) = (R - r)\varsigma(\underline{r}) \tag{17}$$

Here ζ (r) is similar in nature as that given by eqn. (6) with pre assigned exponents. The linear coefficients $D_j^{\pm}$ are determined through the optimization of a suitable time averaged functional due to Löwdin and Mukherjee [41]

$$J(\Phi) = \frac{1}{T}\int_0^T \left\langle \Phi(\underline{r},t) \middle| H_0 + H' - i\frac{\partial}{\partial t} \middle| \Phi(\underline{r},t) \right\rangle dt \tag{18}$$

subject to equation (13). The functional $J(\Phi)$ is expanded and terms up to quadratic in $\delta\Psi^{\pm}$ are retained. The optimization condition

$$\frac{\partial J(\Phi)}{\partial \underline{D}^{\pm}} = 0 \tag{19}$$

yields sets of decoupled linear equations involving D^{+} and D^{-} which are solved by standard technique to obtain the linear coefficients which determine the first order corrections to the ground state wavefunction. Due to finite boundary conditions imposed on the wavefunctions, all the integrals over basis sets are to be evaluated over finite domain R. For each value of cavity radius R, the second order functional is evaluated for a range of external frequency ω. The functional passes through poles at certain values of ω representing double excitations from the ground state. The transition energy to the doubly excited states are obtained from the pole positions and the renormalized first order perturbed two particle functions at poles determine the doubly excited wavefunctions. Such a procedure is repeated for different multipolarity of the one particle perturbation operator ensuring double excitations of different symmetries. Our calculations have been performed only for He atom where relativistic effect is small. Radial correlation is properly taken care of by choosing a reasonable expansion length of the STO's while the angular correlation is ignored here in order to obtain the general pattern for the behavior of the doubly excited states under spherical confinement.

3. RESULTS AND DISCUSSIONS

We have considered the double excitations $1s^2\ :^1S^e \rightarrow nsn's\ :^1S^e$, $npn'p\ :^1D^e$, $ndn'd\ :^1G^e$ for n, $n' \leq 4$ under spherical confinement. Helium atom has been chosen as the prototype for the study to get an insight of the overall behavior of these states under such a confinement which may well reproduce the pattern for other members of the isoelectronic series except for H^- whose behavioral pattern may be different due to strong electron correlation effect. We have restricted the choice of the angular terms of the one particle operators in such a way that the total angular momentum of the generated doubly excited state does not have any contamination from other states generated through angular momentum coupling. For example with a choice of $Y_{00}(1)Y_{00}(2)$, $Y_{11}(1)Y_{11}(2)$ and $Y_{22}(1)Y_{22}(2)$ the respective final states are of S, D and G symmetry without any mixing from other angular momentum states. For the ground state the non linear parameters are chosen as those of Clementi and Roetti [42], the linear coefficients in equation (6) are obtained from the solution of the generalized eigenvalue equation (7) for each radius of confinement. Since both the orbitals are excited from the ground state the quadratic terms in the matrix elements involving the perturbed orbitals $\delta\Psi^{\pm}$ given by equation (15) have no explicit dependence on the ground state function and it acts as a reference level from which the excitation energies are measured. The excitations are essentially dependent on the representation of the $\delta\Psi^{\pm}$. We have chosen 9 parameter representations of the excited s and p orbitals and 8 parameter representation of the d orbitals. Hence the number of unknown coefficients in the expansion of the two particle functions for S, D and G excitations resulting from ss, pp and dd type product basis sets are respectively 45, 45 and 36. The expansion length is adequate to furnish an overall behavior of the double excitations under study. In Table 1 we have listed the excitation energies to the various doubly excited states under study against various confinement radius.

Table 1
Transition energies and Coulomb repulsion term of different doubly excited states of He atom below N = 2, 3 and 4 ionization threshold of the corresponding He^+ for different box radius.

Box Rad. (a.u.)	Pressure (atm.)	Transition Scheme	Transition Energy (a.u.)	Coulomb Repulsion (a.u.)	Bounds
∞	0.0	$1s^2:^1S^e \rightarrow 2s^2:^1S^e$	2.1382 2.1552[a] 2.1259[b] 2.1248[c]	0.2525 0.2526[a]	2.3617 (n=2 S)
		$1s^2:^1S^e \rightarrow 2s3s:^1S^e$	2.2895 2.3085[a] 2.3139[b] 2.3130[c]	0.1153 0.1225[a]	
		$1s^2:^1S^e \rightarrow 2s4s:^1S^e$	2.3244 2.3419[a] 2.3585[c] 2.3604[d]	0.0640 0.0674[a]	
		$1s^2:^1S^e \rightarrow 2p^2:^1D^e$	2.1862 2.2169[a] 2.2009[c] 2.2082[d]	0.2752 0.2794[a]	2.3617 (n=2 P)
		$1s^2:^1S^e \rightarrow 2p3p:^1D^e$	2.3002 2.3198[a] 2.3335[c] 2.3368[d]	0.1105 0.1087[a]	
		$1s^2:^1S^e \rightarrow 2p4p:^1D^e$	2.3284 2.3463[a] 2.3662[c] 2.3677[d]	0.0658 0.0617[a]	
		$1s^2:^1S^e \rightarrow 3s^2:^1S^e$	2.5401 2.5515[a] 2.5496[d]	0.1136 0.1309[a]	2.6395 (n=3 S)
		$1s^2:^1S^e \rightarrow 3s4s:^1S^e$	2.5965 2.6152[a] 2.6235[d]	0.0663 0.0687[a]	
		$1s^2:^1S^e \rightarrow 3p^2:^1D^e$	2.5498 2.5750[a] 2.5595[d]	0.1195 0.1263[a]	2.6395(n=3 P)
		$1s^2:^1S^e \rightarrow 3p4p:^1D^e$	2.5995 2.6190[a] 2.6286[d]	0.0650 0.0636[a]	
		$1s^2:^1S^e \rightarrow 3d^2:^1G^e$	2.5719 2.5917[a] 2.5963[d]	0.1266 0.1261[a]	2.6395 (n=3 D)
		$1s^2:^1S^e \rightarrow 3d4d:^1G^e$	2.6062 2.6239[a]	0.0620 0.0619[a]	
		$1s^2:^1S^e \rightarrow 4s^2:^1S^e$	2.6828 2.6982[a] 2.7017[d]	0.0753 0.0642[a]	2.7367 (n=4 S)
		$1s^2:^1S^e \rightarrow 4p^2:^1D^e$	2.6794 2.7042[a] 2.7047[d]	0.0955 0.0698[a]	2.7367 (n=4 P)
		$1s^2:^1S^e \rightarrow 4d^2:^1G^e$	2.6910 2.7085[a]	0.0708 0.0722[a]	2.7367 (n=4 D)
100	0.01154	$1s^2:^1S^e \rightarrow 2s^2:^1S^e$	2.1383	0.2525	2.3617 (n=2 S)
		$1s^2:^1S^e \rightarrow 2s3s:^1S^e$	2.2895	0.1152	
		$1s^2:^1S^e \rightarrow 2s4s:^1S^e$	2.3242	0.0635	
		$1s^2:^1S^e \rightarrow 2p^2:^1D^e$	2.1862	0.2752	2.3617 (n=2 P)
		$1s^2:^1S^e \rightarrow 2p3p:^1D^e$	2.3002	0.1105	
		$1s^2:^1S^e \rightarrow 2p4p:^1D^e$	2.3286	0.0675	
		$1s^2:^1S^e \rightarrow 3s^2:^1S^e$	2.5403	0.1138	2.6395 (n=3 S)
		$1s:^1S^{e\,2} \rightarrow 3s4s:^1S^e$	2.5966	0.0657	
		$1s^2:^1S^e \rightarrow 3p^2:^1D^e$	2.5500	0.1197	2.6395 (n=3 P)
		$1s^2:^1S^e \rightarrow 3p4p:^1D^e$	2.5996	0.0651	
		$1s^2:^1S^e \rightarrow 3d^2:^1G^e$	2.5719	0.1264	2.6395 (n=3 D)
		$1s^2:^1S^e \rightarrow 3d4d:^1G^e$	2.6062	0.0621	
		$1s^2:^1S^e \rightarrow 4s^2:^1S^e$	2.6846	0.0821	2.7367 (n=4 S)
		$1s^2:^1S^e \rightarrow 4p^2:^1D^e$	2.6814	0.0746	2.7367 (n=4 P)
		$1s^2:^1S^e \rightarrow 4d^2:^1G^e$	2.6913	0.0714	2.7367 (n=4 D)

contd. table 1

Box Rad. (a.u.)	Pressure (atm.)	Transition Scheme	Transition Energy (a.u.)	Coulomb Repulsion (a.u.)	Bounds
25	3.57640	$1s^2.{}^1S^e \rightarrow 2s^2.{}^1S^e$	2.1389	0.2530	2.3616 (n=2 S)
		$1s^2.{}^1S^e \rightarrow 2s3s.{}^1S^e$	2.2898	0.1158	
		$1s^2.{}^1S^e \rightarrow 2s4s.{}^1S^e$	2.3326	0.0890	
		$1s^2.{}^1S^e \rightarrow 2p^2.{}^1D^e$	2.1862	0.2752	2.3616 (n=2 P)
		$1s^2.{}^1S^e \rightarrow 2p3p.{}^1D^e$	2.3004	0.1127	
		$1s^2.{}^1S^e \rightarrow 2p4p.{}^1D^e$	2.3404	0.0978	
		$1s^2.{}^1S^e \rightarrow 3s^2.{}^1S^e$	2.5434	0.1241	2.6394 (n=3 S)
		$1s^2.{}^1S^e \rightarrow 3s4s.{}^1S^e$	2.6015	0.0783	
		$1s^2.{}^1S^e \rightarrow 3p^2.{}^1D^e$	2.5540	0.1336	2.6394 (n=3 P)
		$1s^2.{}^1S^e \rightarrow 3p4p.{}^1D^e$	2.6059	0.0814	
		$1s^2.{}^1S^e \rightarrow 3d^2.{}^1G^e$	2.5719	0.1269	2.6394 (n=3 D)
		$1s^2.{}^1S^e \rightarrow 3d4d.{}^1G^e$	2.6135	0.0839	
		$1s^2.{}^1S^e \rightarrow 4s^2.{}^1S^e$	2.6830	0.0679	2.7369 (n=4 S)
		$1s^2.{}^1S^e \rightarrow 4p^2.{}^1D^e$	2.6866	0.0712	2.7368 (n=4 P)
		$1s^2.{}^1S^e \rightarrow 4d^2.{}^1G^e$	2.6917	0.0742	2.7367 (n=4 D)
20	9.43185	$1s^2.{}^1S^e \rightarrow 2s^2.{}^1S^e$	2.1393	0.2535	2.3616 (n=2 S)
		$1s^2.{}^1S^e \rightarrow 2s3s.{}^1S^e$	2.2911	0.1208	
		$1s^2.{}^1S^e \rightarrow 2s4s.{}^1S^e$	2.3517	0.1135	
		$1s^2.{}^1S^e \rightarrow 2p^2.{}^1D^e$	2.1862	0.2752	2.3616 (n=2 P)
		$1s^2.{}^1S^e \rightarrow 2p3p.{}^1D^e$	2.3025	0.1208	
		$1s^2.{}^1S^e \rightarrow 2p4p.{}^1D^e$	2.3610	0.1234	
		$1s^2.{}^1S^e \rightarrow 3s^2.{}^1S^e$	2.5886	0.1645	2.6394 (n=3 S)
		$1s^2.{}^1S^e \rightarrow 3s4s.{}^1S^e$	2.6176	0.1077	
		$1s^2.{}^1S^e \rightarrow 3p^2.{}^1D^e$	2.5479	0.1214	2.6394 (n=3 P)
		$1s^2.{}^1S^e \rightarrow 3p4p.{}^1D^e$	2.5905	0.1786	
		$1s^2.{}^1S^e \rightarrow 3d^2.{}^1G^e$	2.5724	0.1294	2.6394 (n=3 D)
		$1s^2.{}^1S^e \rightarrow 3d4d.{}^1G^e$	2.6280	0.1054	
		$1s^2.{}^1S^e \rightarrow 4s^2.{}^1S^e$	2.6864	0.0809	2.7396 (n=4 S)
		$1s^2.{}^1S^e \rightarrow 4p^2.{}^1D^e$	2.6878	0.0870	2.7389 (n=4 P)
		$1s^2.{}^1S^e \rightarrow 4d^2.{}^1G^e$	2.6918	0.0978	2.7378 (n=4 D)
10	228.259	$1s^2.{}^1S^e \rightarrow 2s^2.{}^1S^e$	2.1383	0.2557	2.3613 (n=2 S)
		$1s^2.{}^1S^e \rightarrow 2s3s.{}^1S^e$	2.2941	0.3809	
		$1s^2.{}^1S^e \rightarrow 2s4s.{}^1S^e$	2.3740	0.2189	
		$1s^2.{}^1S^e \rightarrow 2p^2.{}^1D^e$	2.1878	0.2819	2.3613 (n=2 P)
		$1s^2.{}^1S^e \rightarrow 2p3p.{}^1D^e$	2.3863	0.2257	
		$1s^2.{}^1S^e \rightarrow 3s^2.{}^1S^e$	2.6066	0.1513	2.6616 (n=3 S)
		$1s^2.{}^1S^e \rightarrow 3s4s.{}^1S^e$	2.6556	0.2187	
		$1s^2.{}^1S^e \rightarrow 3p^2.{}^1D^e$	2.6002	0.1663	2.6548 (n=3 P)
		$1s^2.{}^1S^e \rightarrow 3p4p.{}^1D^e$	2.6519	0.2417	
		$1s^2.{}^1S^e \rightarrow 3d^2.{}^1G^e$	2.6159	0.1767	2.6454 (n=4 D)
		$1s^2.{}^1S^e \rightarrow 3d4d.{}^1G^e$	2.8185	0.1894	
8	694.369	$1s^2.{}^1S^e \rightarrow 2s^2.{}^1S^e$	2.1425	0.2734	2.3619 (n=2 S)
		$1s^2.{}^1S^e \rightarrow 2s3s.{}^1S^e$	2.2093	0.4192	
		$1s^2.{}^1S^e \rightarrow 2s4s.{}^1S^e$	2.4765	0.2529	
		$1s^2.{}^1S^e \rightarrow 2p^2.{}^1D^e$	2.1956	0.2975	2.3614 (n=3 P)
		$1s^2.{}^1S^e \rightarrow 2p3p.{}^1D^e$	2.4818	0.2805	
		$1s^2.{}^1S^e \rightarrow 3s^2.{}^1S^e$	2.7678	0.1803	2.7220 (n=3 S)
		$1s^2.{}^1S^e \rightarrow 3p^2.{}^1D^e$	2.7283	0.1878	2.6981 (n=3 P)
		$1s^2.{}^1S^e \rightarrow 3d^2.{}^1G^e$	2.6839	0.2097	2.6642 (n=3 D)
6	3219.36	$1s^2.{}^1S^e \rightarrow 2s^2.{}^1S^e$	2.1943	0.3057	2.3739 (n=2 S)
		$1s^2.{}^1S^e \rightarrow 2s3s.{}^1S^e$	2.3032	0.3457	
		$1s^2.{}^1S^e \rightarrow 2p^2.{}^1D^e$	2.2373	0.3395	2.3666 (n=2 P)
		$1s^2.{}^1S^e \rightarrow 3s^2.{}^1S^e$	2.7735	0.3169	
		$1s^2.{}^1S^e \rightarrow 3p^2.{}^1D^e$	2.7203	0.3532	2.8532 (n=3 P)
5	17951.0	$1s^2.{}^1S^e \rightarrow 2s^2.{}^1S^e$	2.3030	0.3406	2.4063 (n–2 S)
		$1s^2.{}^1S^e \rightarrow 2p^2.{}^1D^e$	2.3062	0.3812	2.3821 (n=2 P)
4	86992.5	$1s^2.{}^1S^e \rightarrow 2s^2.{}^1S^e$	2.4963	0.5488	2.5117 (n=2 S)
		$1s^2.{}^1S^e \rightarrow 2p^2.{}^1D^e$	2.4788	0.4501	2.4329 (n=2 P)

[a][43], [b][44], [c][45], [d][46]

We start with a sufficiently large radius 1000 a.u. to represent the free system and subsequently reducing the radius in such a manner that effect of strong confinement is being imposed upon. The excitation energies are obtained from the position of the poles of the variational functional given by equation (18) with respect to the frequency of the harmonic perturbation. From Table 1 we notice that for the free system our results compare favorably with existing available data. Some of the more recent calculations indicate the positions of the doubly excited states [47, 48] only without mentioning the ground state energy. We have calculated the doubly excited state energies from our data and find that the positions of the doubly excited $^1S^e$ states for $2s^2$, $2s3s$, $2s4s$, $3s^2$, $3s4s$ and $4s^2$ are respectively 0.7235, 0.5722, 0.5373, 0.3216, 0.2652 and 0.1789 a.u. compared to 0.7779, 0.5899, 0.5449, 0.3535, 0.2811 and 0.2010 a.u. as obtained by B*ü*rgers *et al.* [47] while for $2p^2$:$^1D^e$ state our result 0.6621 a.u. has to be compared with 0.7018 a.u. due to Kar and Ho [48]. The discrepancy arises due to neglect of angular correlation in our calculation as well as due to the specific choice of our reference ground state level. The result obtained by Chakraborty and Ho [34] for the free $2s^2$:$^1S^e$ state is identical with that of B*u*¨rgers *et.al.* [47]. The renormalized perturbed functions at pole positions furnish the representation of the corresponding doubly excited state wavefunction in terms of product basis. These wavefunctions have been used to calculate the matrix element of the Coulomb repulsion term $\frac{1}{r_{12}}$. The spherical confinement generates a thermodynamic pressure within the system which can be calculated by the standard expression [49]

$$P = \frac{1}{4\pi R^2}\left[2E_0 - \langle V \rangle\right] \tag{20}$$

where E_0 is the ground state energy $<V>$ is the potential energy and R is the radius of confinement. The corresponding pressure calculated for each R value is also listed in Table 1. The doubly excited $nln'l'$ ($n, n' \geq 2$) states are bounded below the corresponding ionization threshold of He^+ with principal quantum number n. Due to spherical confinement the accidental degeneracy of hydrogenic levels is lifted. This lifting is apparent at sufficiently low values of the radius of confinement. In our study of the He^+ ion using time dependent perturbation theory we have estimated the energy levels for different orbital angular momentum states for a given principal quantum number n which takes the values 2, 3 and 4 respectively. Specifically we calculated the bounds for S and P levels for $n = 2$ while for $n = 3$ and 4 the bounds for S, P and D levels have been evaluated. The respective bounds have been listed in Table 1. To get a feeling of the behavior of the different bounds we have plotted in figure 1 the respective bounds for n=2 and n=3 levels against the radius of confinement.

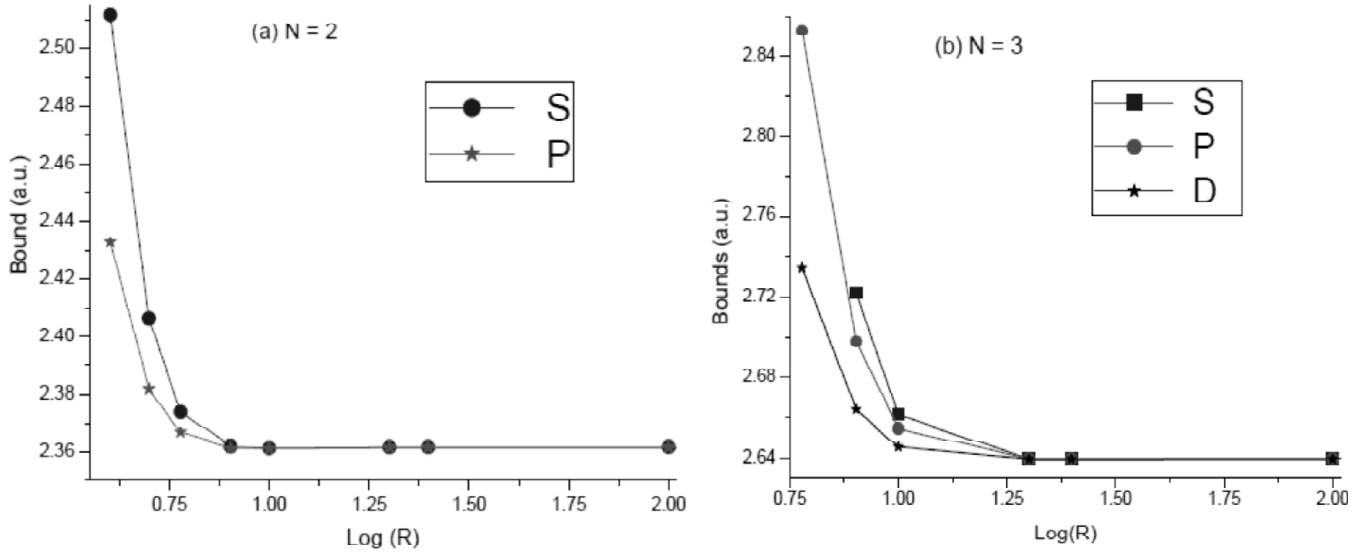

Figure 1: Plot of the bounds for He^+ below (a) N = 2 and (b) N = 3 against radius of confinement.

The plots clearly demonstrate the lifting of the degeneracy's of He^+ ion at strong confinement and their enhanced values at larger confinements. It is also noted from figure 1 that at certain radius some of the bounds exist while others are not. Such thresholds calculated for He^+ at each R and n values, have also been listed in Table 1 in order to have a ready reference. Double excitation energies of the states lying above the ionization threshold for any given R are not listed in the Table as they are unstable. From the host of data collected in Table 1 we observe a general tendency of increase of the transition energy as well as the Coulomb repulsion with decrease of radius of confinement R. At R = 10.0 a u there is a slight reduction of the transition energy $1s^2 \rightarrow 2s^2$ departing from the general trend. This feature is difficult to resolve at the present state of calculations and needs more sophisticated fully correlated studies of the problem. Figure 2 represents plots of the double excitation energies $1s^2 \rightarrow 2s^2$, $2s3s$ and $2s4s$ against radius of confinement R. Figures 3 and 4 represent such plots for the double excitation energies $1s^2 \rightarrow 2p^2$ $2p3p$ $3d^2$ and $3d4d$ respectively against R for He.

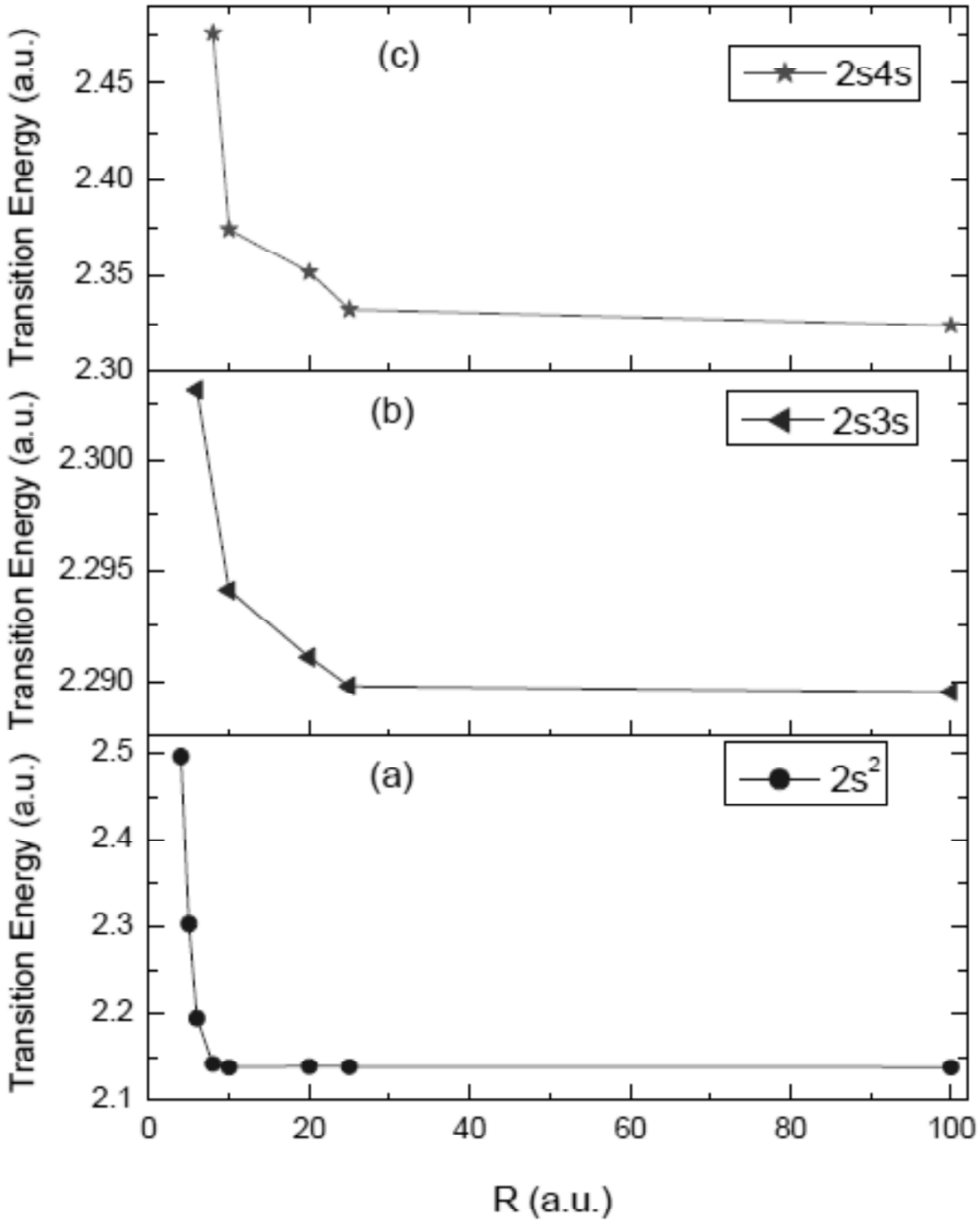

Figure 2: Plot of double excitation energy against confinement radius R (a) $1s^2 \rightarrow 2s^2$; (b) $1s^2 \rightarrow 2s3s$; (c) $1s^2 \rightarrow 2s4s$

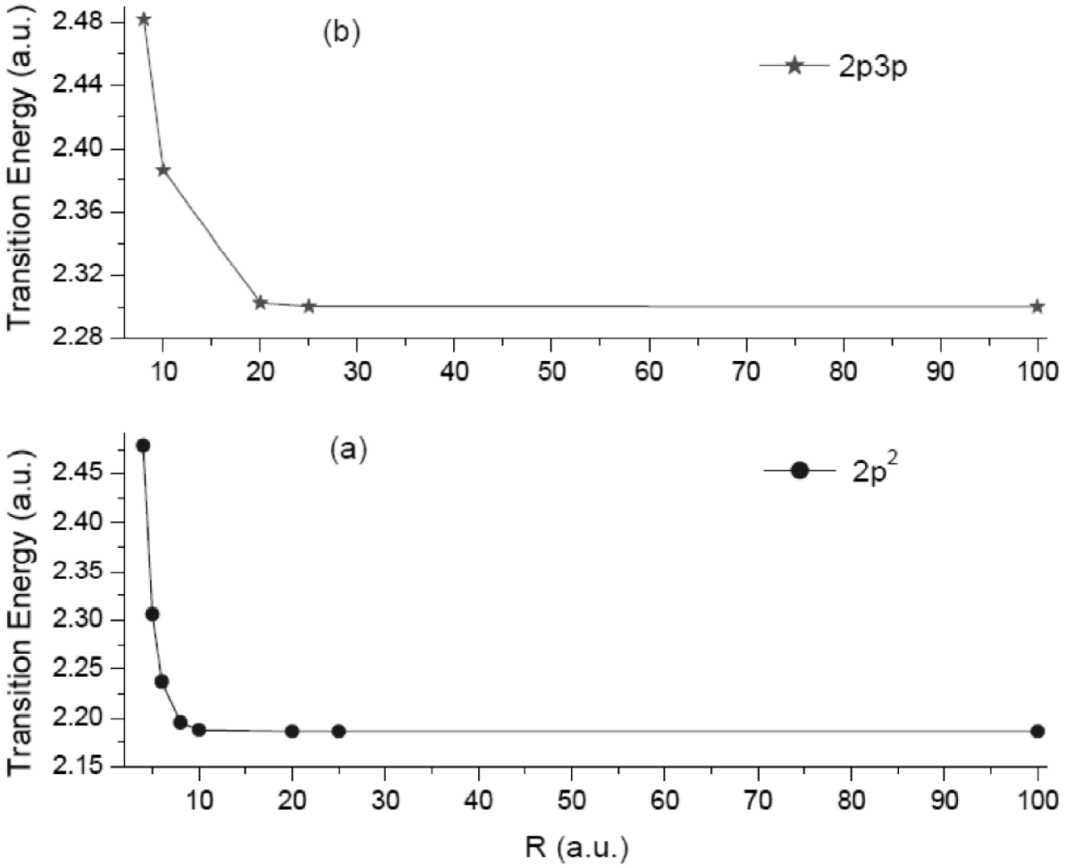

Figure 3: Plot of double excitation energy against confinement radius R (a) $1s^2 \rightarrow 2p^2$; (b) $1s^2 \rightarrow 2p3p$ for He

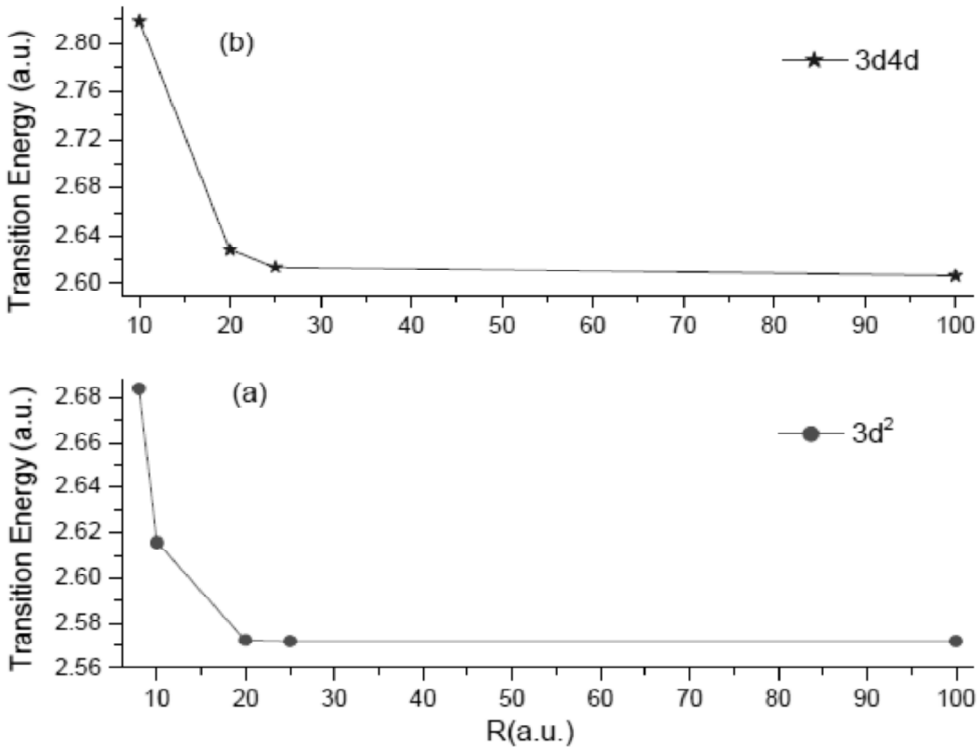

Figure 4: Plot of double excitation energy against confinement radius R (a) $1s^2 \rightarrow 3d^2$; (b) $1s^2 \rightarrow 3d4d$ for He

In all the cases we observe systematic trend of the double excitation energies against the radius of confinement. The plot for the double excitation energy $1s^2 \rightarrow 2p4p$ is omitted as this state goes beyond ionization threshold for most of the confining radii as reflected in Table 1. In order to have a feeling for the density profiles of the doubly excited states for different radii of confinement the radial density distribution $r_1^2 r_2^2 |\Psi(r_1, r_2)|^2$ against r_1 and r_2 has been plotted for the respective states $2s^2$, $3s^2$, $4s^2$, $2p^2$, $3p^2$, $4p^2$, $3d^2$ and $4d^2$ at R = 1000.0 a.u. which corresponds to the free system and at R =10.0 a.u. or 20.0 a.u. depending on the stability of the states. R=20.0 a.u. has been used only for $4s^2$, $4p^2$ and $4d^2$ states. Such plots are distributed over the Figures 5 to 12.

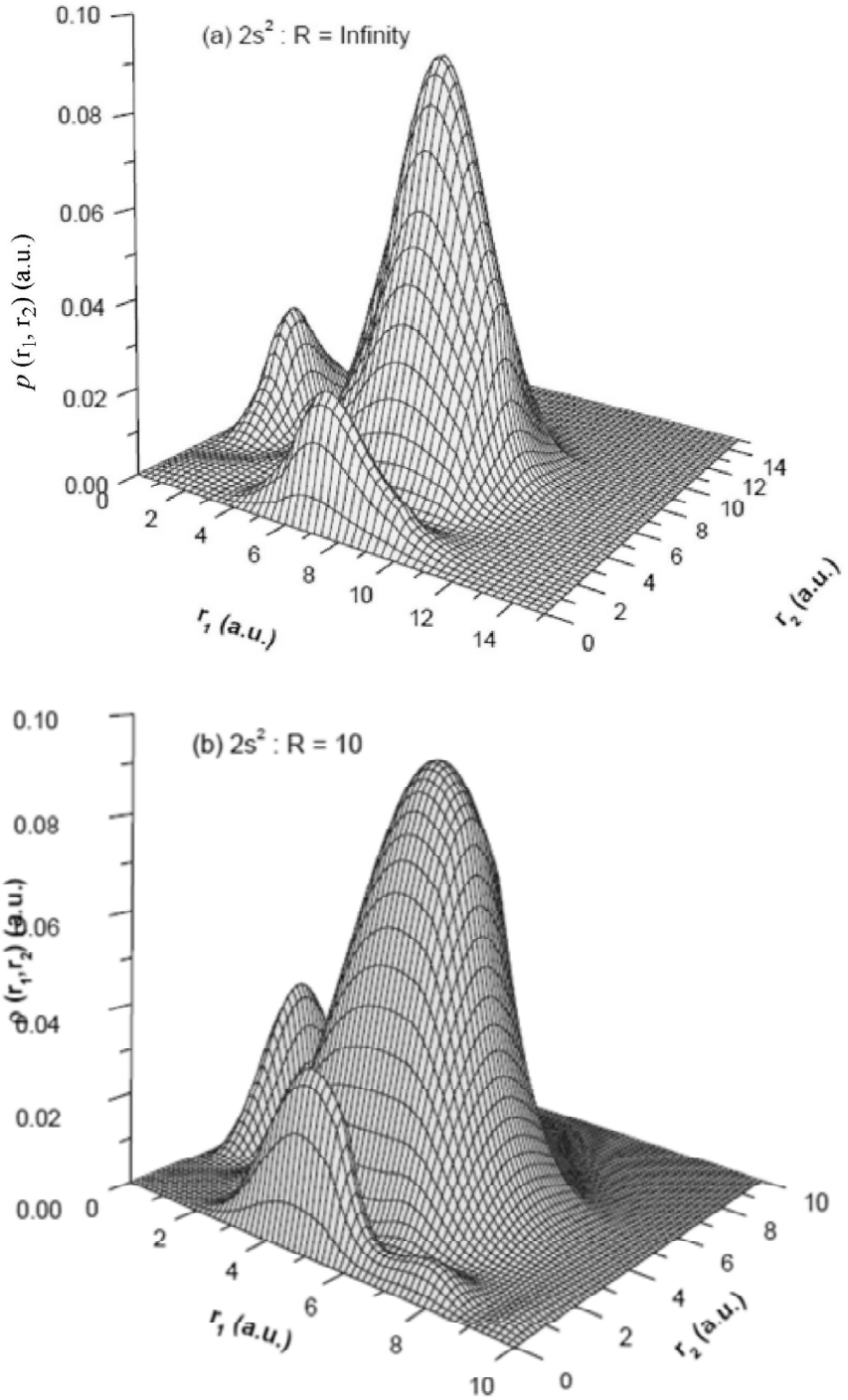

Figure 5: Plot of two particle density ρ (r_1, r_2) against r_1 and r_2 for the doubly excited $2s^2$ state at (a) R = Infinity and (b) R = 10 a.u for He

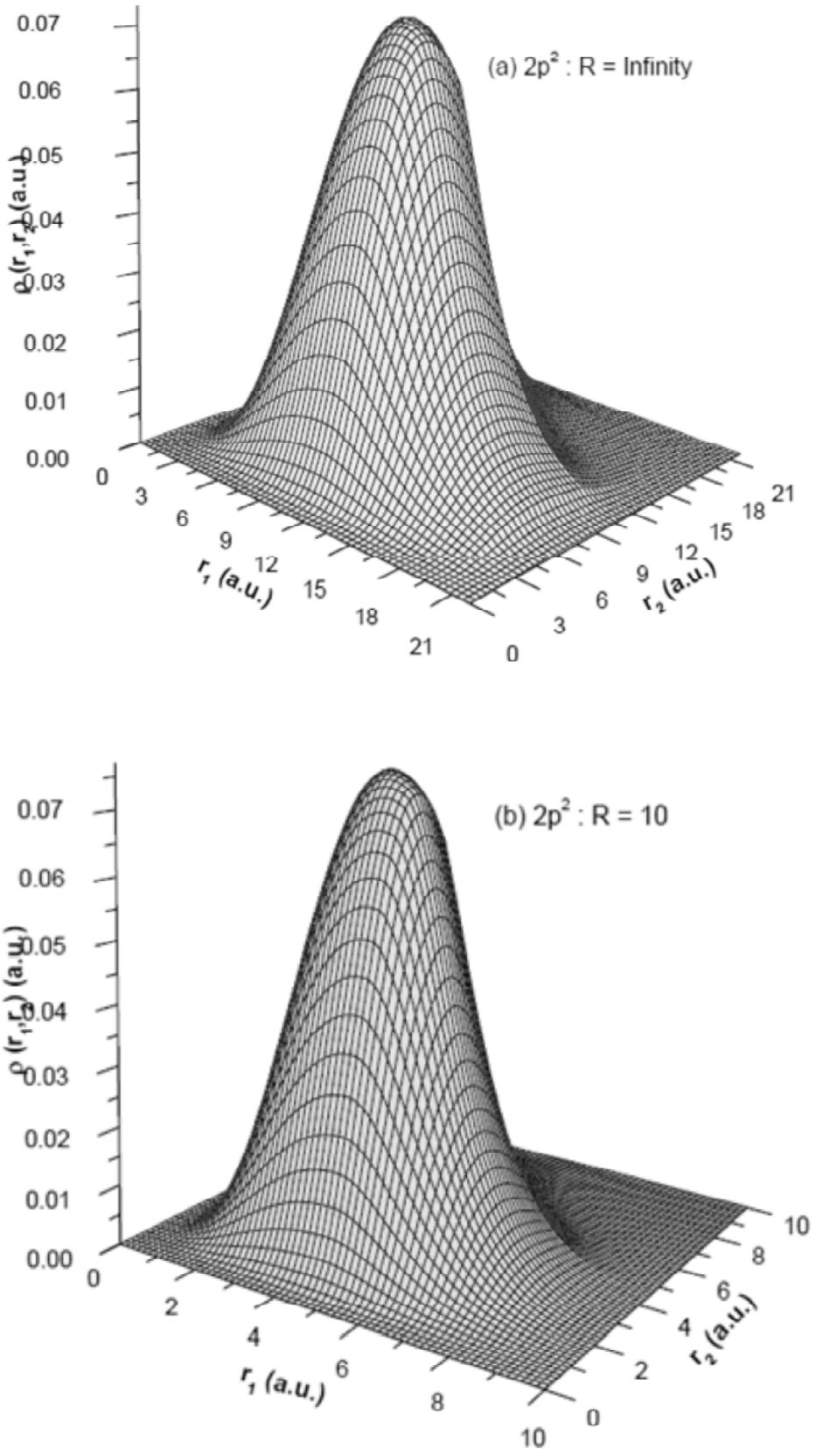

Figure 6: Plot of two particle density ρ (r_1, r_2) against r_1 and r_2 for the doubly excited $2p^2$ state at (a) R = Infinity and (b) R = 10 a.u. for He

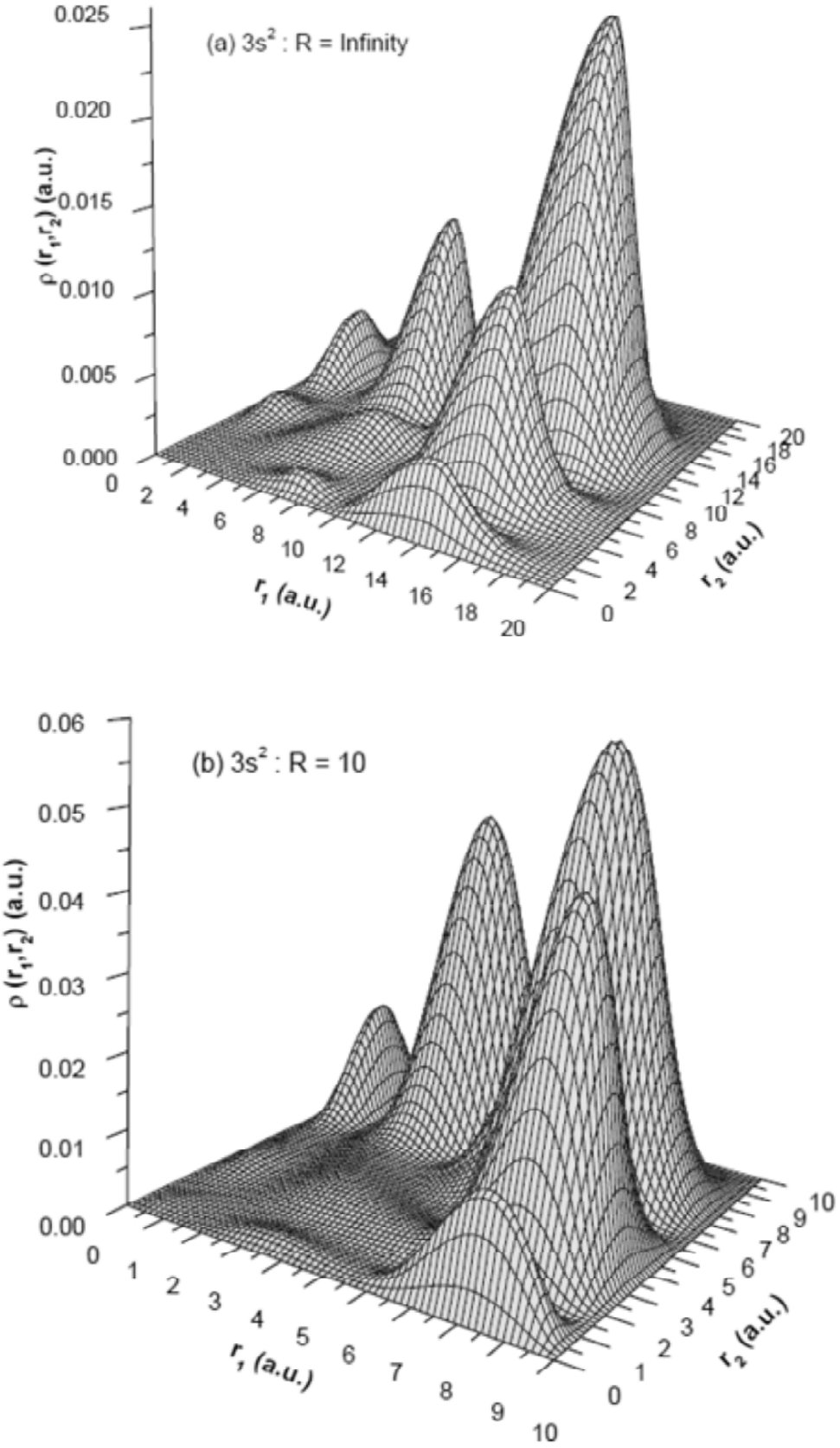

Figure 7: Plot of two particle density ρ (r_1, r_2) against r_1 and r_2 for the doubly excited $3s^2$ state at (a) R = Infinity and (b) R = 10 a.u. for He

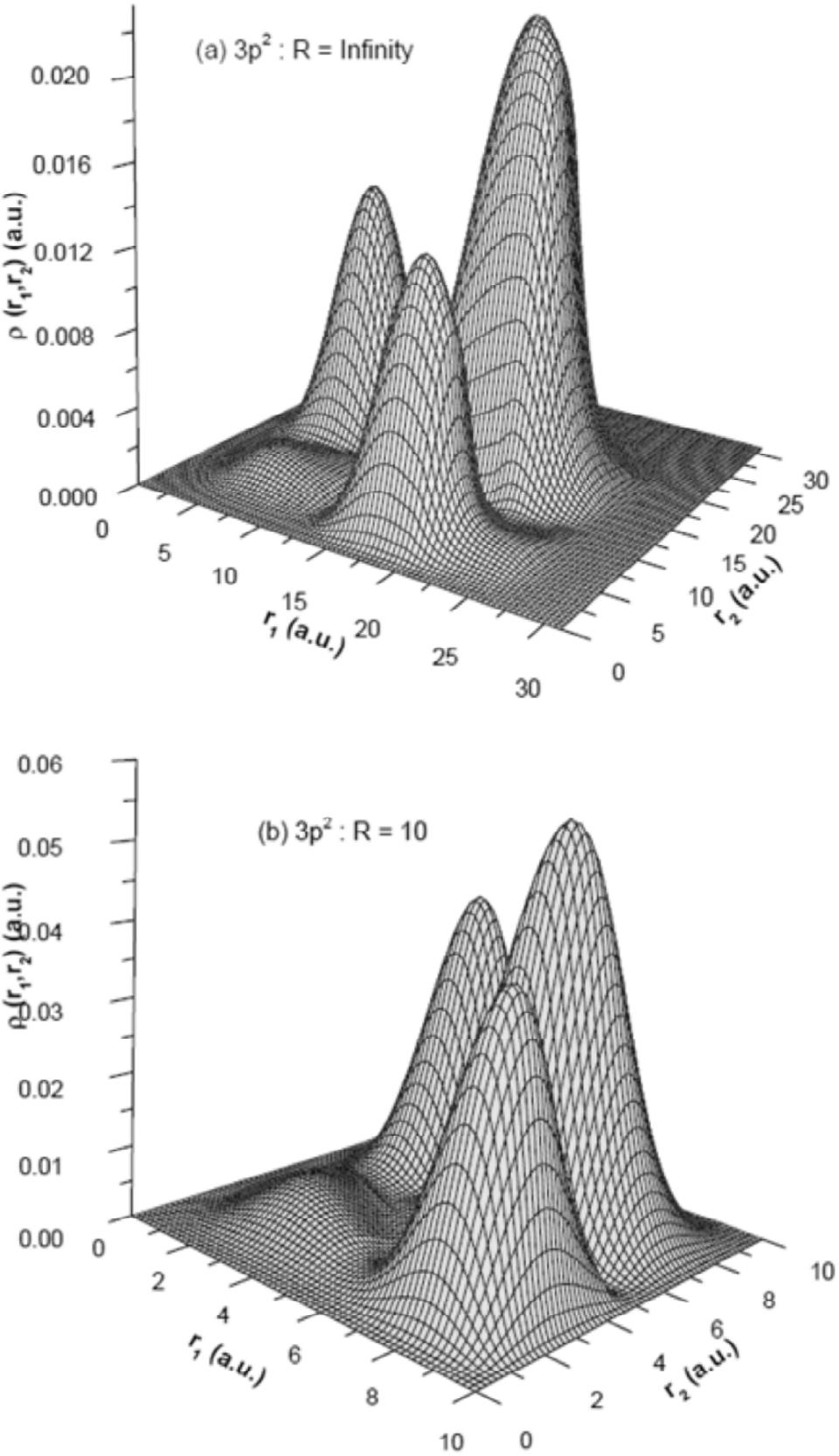

Figure 8: Plot of two particle density ρ (r_1, r_2) against r_1 and r_2 for the doubly excited $3p^2$ state at (a) R = Infinity and (b) R = 10 a.u. for He

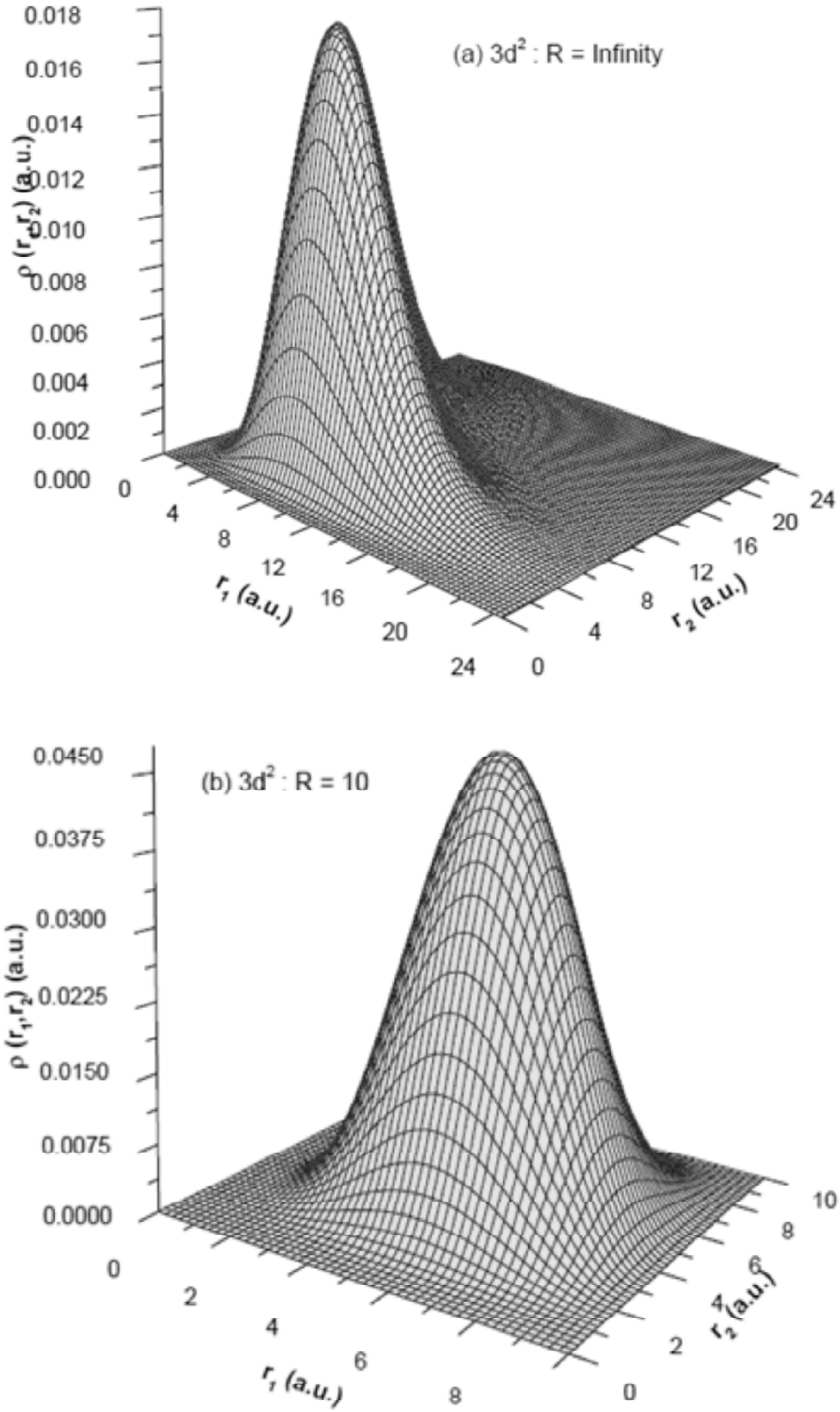

Figure 9: Plot of two particle density ρ (r_1, r_2) against r_1 and r_2 for the doubly excited $3d^2$ state at (a) R = Infinity and (b) R = 10 a.u. for He

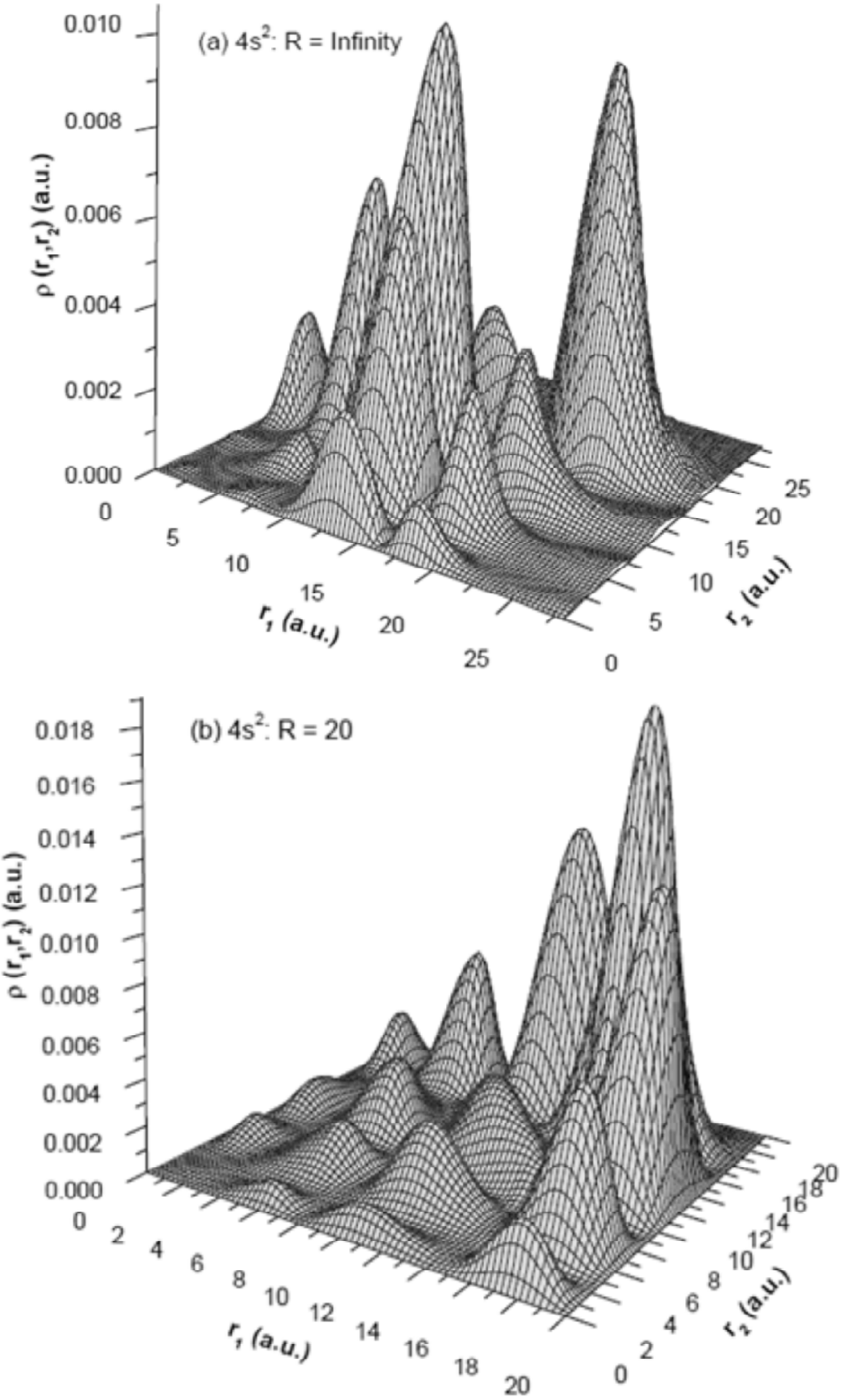

Figure 10: Plot of two particle density ρ (r_1, r_2) against r_1 and r_2 for the doubly excited $4s^2$ state at (a) R = Infinity and (b) R = 20 a.u. for He

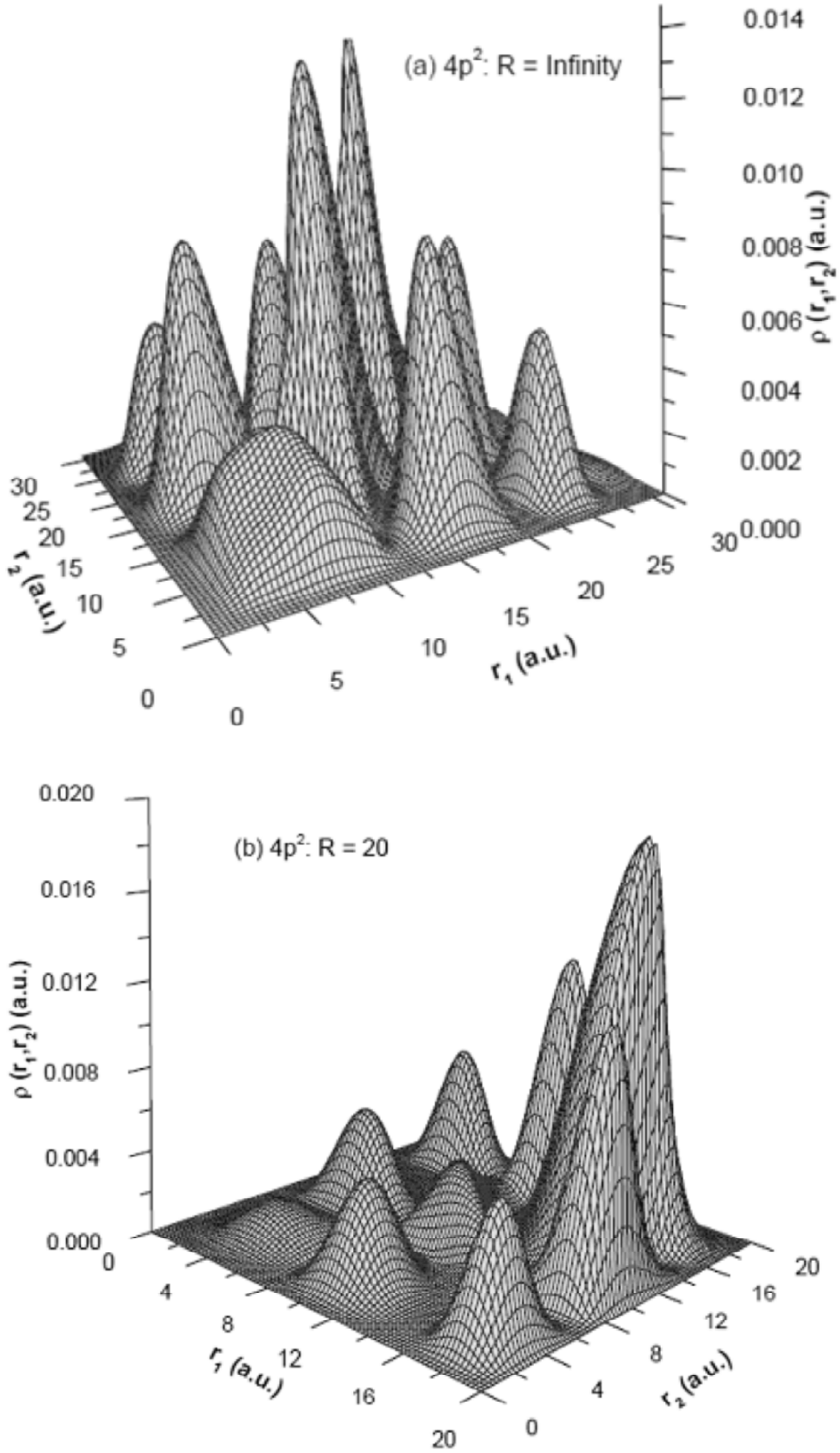

Figure 11: Plot of two particle density ρ (r_1, r_2) against r_1 and r_2 for the doubly excited $4p^2$ state at (a) R = Infinity and (b) R = 20 a.u. for He

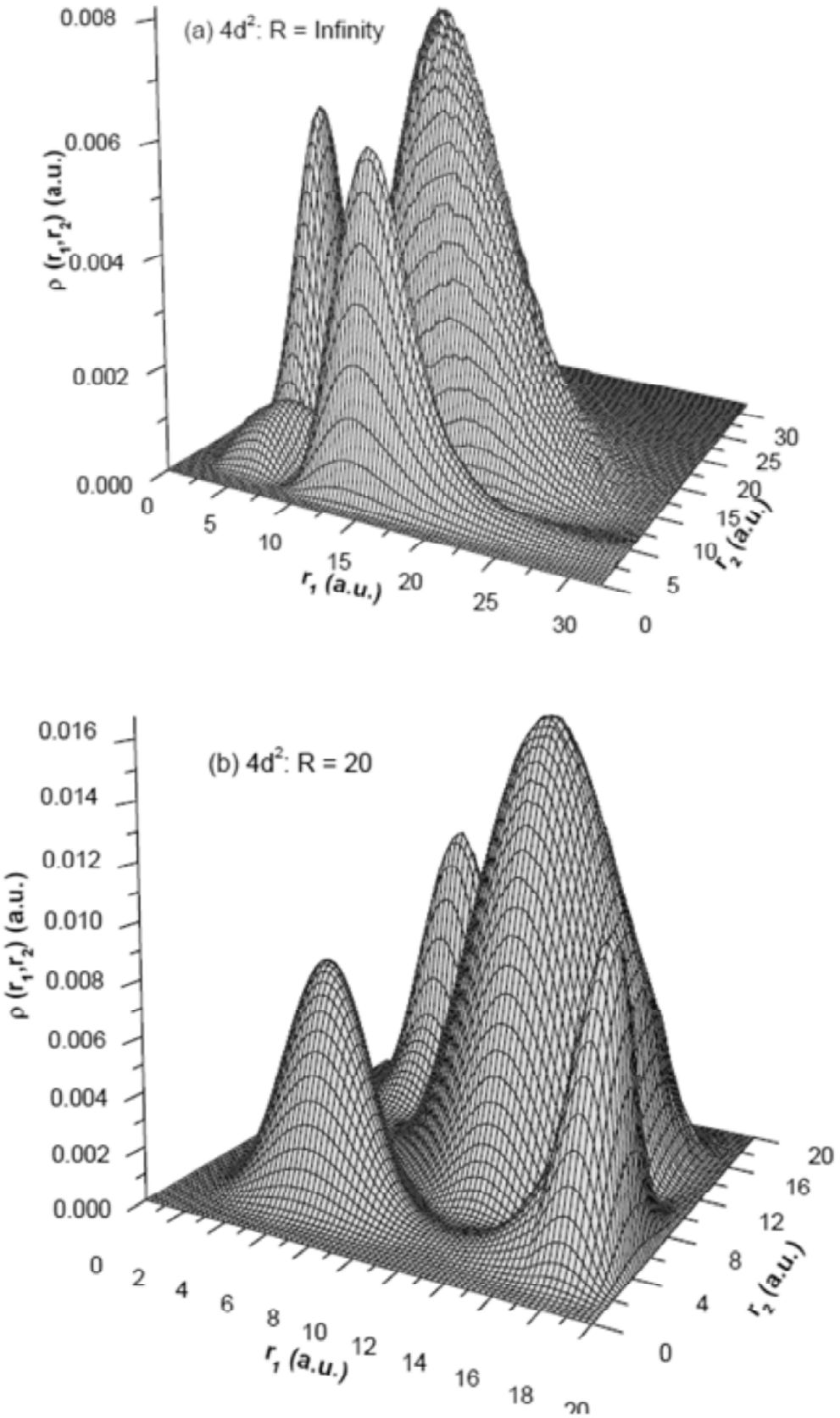

Figure 12: Plot of two particle density ρ (r_1, r_2) against r_1 and r_2 for the doubly excited $4d^2$ state at (a) R = Infinity and (b) R = 20 a.u. for He

The three dimensional plots of the density profiles clearly indicate the effect of confinement through enhancement of the peak heights with reduction of spatial extension with respect to r_1 and r_2 maintaining the nature of the nodes. Such density profiles for the doubly excited states have been reported for the first time.

4. CONCLUSION

Doubly excited states of several symmetries of *He* atom under spherical confinement have been studied and their density profiles are analyzed. Behavioral pattern for such excitations under strong confinement indicates that the energy of a doubly excited state increases as the radius of confinement decreases. Full understanding in this direction necessitates the evaluation and analysis of their positions using fully correlated methods.

Acknowledgments

PKM is thankful to Alexander von Humboldt Foundation for sponsoring a short stay in Germany to complete the project work. He is also thankful to the Department of Science and Technology (DST), Government of India for support through the research grant no. SR/S2/LOP-22/2009. PKM is also thankful to the Inter University Accelerator Centre IUAC) New Dehi for their Associateship. PM is partially supported under Special Assistance Programme of the University Grants Commission, New Delhi through Grant No F 510/4/DRS/2009 SAP-I.

References

[1] A. Michels, J de Boer and A. Bijl, *Physica*, **4**, 981, (1937).

[2] A. Sommerfeld and H Welker, *Ann. Phys.*, **32**, 56, (1938).

[3] P. A. Jacobs, Carboniogenic Activity of Zeolites Elsevier, *Amsterdam* (1997).

[4] Z. K. Tang Y. Nozue and T. Goto, *J. Phys Soc Japan*, **61** 2943, (1992).

[5] H. W. Kroto, J. R. Heath, S. C. O. Brian, R. F. Curl and R. E. Smalley, *Nature*, **318**, 162, (1985).

[61 J. Cioslowski and E. D. Fleischmann, J Chem Phys, **94**, 3730, (1991).

[7] A. S. Baltenkov, *J. Phys. B*, **32**, 2745, (1999).

[8] J. P. Connerade, V. K. Dolmatov, P. A. Lakshmi and S. T. Manson, *J. Phys. B*, **32**, L239, (1999).

[9] J. P. Connerade, V. K. Dolmatov and S T Manson, *J. Phys. B*, **32**, L395, (1999).

[10] C. Reichhard, Solvents and Solvent Effects in Organic Chemistry V C H Germany Weinhein (1988).

[11] B. Mennucci, R. Cami Ed. Continuum Solvation Models in Chemical physics Wiley (2007).

[12] S. Canuto Ed., Solvation Effects on Molecules and Biomolecules Computational methods and Applications Springer (2008).

[13] J. P. Connerade, J. Alloy Relat. *Compounds*, **255**, 79, (1997).

[14] W. Jaskolski, Phys. Rept., **2**, 11, (1996).

[15] A. N. Sil, S. Canuto and P. K. Mukherjee, Adv. Quant. Chem., **58**, 115, (2009).

[16] J. C. A. Boeyens, *J. Chem. Soc. Farad. Trans.*, **90**, 3377, (1994).

[17] S. R. de Groot and C. A. Ten Seldam, *Physica*, **12**, 669, (1946).

[18] R. B. Dingle, Proc. Camb. Phil. Soc., **49**, 103, (1953).

[19] A. D. Buckingham and K. P. Lawley, Mol. Phys., **3**, 219, (1960).

[20] D. Suryanarayana and J. A. Weil, *J. Chem. Phys.*, **64**, 510, (1976).

[21] E. V. Ludena, *J. Chem. Phys.*, **66**, 46, (1977).

[22] E. Lee-Koo and S. Rubinstein, *J. Chem. Phys.*, **71**, 351, (1979).

[23] G. A. Arteca, F. M. Fernandez and E. A. Castro, *J. Chem. Phys.*, **80** 1569, (1984).

[24] J. Gorecki and W. Bayers Brown, *J. Phys. B*, **20**, 5953, (1987).

[25] J. Gorecki and W. Bayers Brown, J. Phys. B, **22**, 2659, (1989).

[26] P. L. Goodfriend, *J. Phys. B*, **23**, 1373, (1990).

[27] J. L. Marin and S. A. Cruz, *Am J. Phys.*, **59**, 931, (1991).

[28] S. Goldman and C. Joslin, J. Phys. Chem., **96**, 6021, (1992).

[29] R. Dutt, A. Mukherjee and Y. P. Varshni, Phys. Rev. A, **52**, 1750, (1995).

[30] Y. P. Varshni, J. Phys. B, **30** L5, 9, (1997).

[31] Y. P. Varshni, J. Phys. B, **31**, 2, 49, (1998).

[32] A. Banerjee, K. D. Sen, J. Garza and R. Vargas, *J. Chem. Phys*., **116**, 4054, (2002).

[33] Y. S. Huang, C. C. Yang and S-S Liaw, *Phys. Rev. A*, **60**, 5, (1999).

[34] J. L. Marin and S. A. Cruz, *J. Phys. B*, **24**, 2, 99, (1991).

[35] J. P. Connerade and V. K. Dolmatov, *J. Phys. B*, **31**, 3557, (1998).

[36] J. P. Connerade V. K. Dolmatov and P. A. Lakshmi, *J. Phys. B*, **33**, 251, (2000).

[37] J. K. Saha T. K. Mukherjee P. K. Mukherjee and B. Fricke, Eur. Phys. J D, **62** 2054 (2011) *ibid*. **66**, 43, (2012).

[38] S. Sen P. Mandal and P. K. Mukherjee, *Phys. Plas*., **19**, 033501, (2012).

[39] S. Chakraborty and Y. K. Ho, Phys. Rev. A, **84**, 032515, (2011).

[40] H. Nguyen M. König D. Benredjem M. Caby and G. Coulaud, *Phys. Rev. A* **33**, 1279, (1986).

[41] P. O. Löwdin and P. K. Mukherjee, *Chem. Phys. Lett*., **14**, 1, (1972).

[42] E. Clementi and C. Roetti, At. Data Nucl. Data Tables, **14**, 177, (1974).

[43] D. Ray and P. K. Mukherjee, *J. Phys. B*, **24**, 1241, (1991).

[44] Y. K. Ho, *Phys. Rev. A*, **23**, 2137, (1981).

[45] P. J. Hicks and J. Comer, *J. Phys. B*, **8** 1866, (1975).

[46] D. R. Herrick and O. Sinanoglu, *Phys. Rev. A*, **11**, 97, (1975).

[47] A. Bürgers D. Wintgen and J-M Rost, *J. Phys. B*, **28**, 3163, (1995).

[48] S. Kar and Y. K. Ho, *Phys. Scr.*, **75**, 13, (2007).

[49] J. O. Hirschfelder, C. P. Curtis and R. B. Bird, Molecular Theory of Gases and Liquids, John Wiley and Sons New York p 265 (1954).